Dynein catch bond as a mediator of codependent bidirectional cellular transport

Palka Puri,[1,2] Nisha Gupta,[3] Sameep Chandel,[3] Supriyo Naskar,[1,4] Anil Nair,[5] Abhishek Chaudhuri,[3] Mithun K. Mitra,[1,*] and Sudipto Muhuri[5,†]

[1]*Department of Physics, IIT Bombay, Mumbai 400076, India*

[2]*Institute for Nonlinear Dynamics, Georg August University of Goettingen, Goettingen 37077, Germany*

[3]*Indian Institute of Science Education and Research Mohali, Punjab 140306, India*

[4]*Department of Physics, Indian Institute of Science, Bangalore 560012, India*

[5]*Department of Physics, Savitribai Phule Pune University, Ganeshkhind, Pune 411007, India*

Abstract

Intracellular bidirectional transport of cargo on Microtubule filaments is achieved by the collective action of oppositely directed *dynein* and *kinesin* motors. Experimental investigations probing the nature of bidirectional transport have found that in certain cases, inhibiting the activity of one type of motor results in an overall decline in the motility of the cellular cargo in both directions. This somewhat counter-intuitive observation, referred to as *paradox of codependence* is inconsistent with the existing paradigm of a mechanistic *tug-of-war* between oppositely directed motors. Existing theoretical models do not take into account a key difference in the functionality of kinesin and dynein. Unlike kinesin, dynein motors exhibit *catchbonding*, wherein the unbinding rates of these motors from the filaments are seen to decrease with increasing force on them. Incorporating this *catchbonding* behavior of dynein in a theoretical model and using experimentally relevant measures characterizing cargo transport, we show that the functional divergence of the two motors species manifests itself as an internal regulatory mechanism for bidirectional transport and resolves the *paradox of codependence*. Our model reproduces the key experimental features in appropriate parameter regimes and provides an unifying framework for bidirectional cargo transport.

* mithun@phy.iitb.ac.in

† sudipto@physics.unipune.ac.in

INTRODUCTION

Bidirectional transport is ubiquitous in nature in the context of intracellular transport [1–13]. Within the cell, organelles such as mitochondria, phagosomes, endosomes, lipid droplets and vesicles are transported by sets of oppositely directed motor proteins [1, 7, 9–11, 14–24]. The transport itself happens bidirectionally, wherein *dynein* and *kinesin* motors carry the cellular cargo on microtubule(MT) filaments [1, 15]. While the phenomenon of bidirectional transport has been well studied experimentally under both *in-vitro* and *in-vivo* conditions for variety of different systems [1, 25], the underlying mechanism by which the motors involved in bidirectional transport are able to achieve regulated long distance transport is far from clear and is a subject of much debate [1, 7, 25–29].

A theoretical framework proposed to explain the bidirectional transport is based on the *tug-of war* hypothesis [1, 8, 15, 25, 28, 30, 31]. The basic underlying premise of this hypothesis is that the motors act independently, stochastically binding to and unbinding from the filament and mechanically interacting with each other through the cargo that they carry (Fig. 1a) [25, 28, 30]. The resultant motion arises due to the competition between the oppositely directed motors with the direction of transport being determined by the stronger set of motors [28, 30]. Diverse experiments have provided support for this mechanical tug-of-war picture, with the observed features matching with the simulated cargo trajectories [15, 28, 32–36]. Studies on endosomal transport in *D. discoideum* cells and on mitochondria in mitral cell dendrites have observed elongation of cargo when attached to both motor species, supporting the hypothesis that oppositely directed mechanical forces act simultaneously on the cargo [37, 38].

While the stochastic *tug-of-war* model has proven to be effective in understanding many transport properties, there remain a large class of experiments whose findings are incompatible with the predictions of this model [25, 39–53]. Since the oppositely directed motors of *dynein* and *kinesin* are involved in mechanical competition, the *tug-of-war* model predicts that inhibiting the activity of one kind of motor would lead to enhancement of motility in the opposite direction. However, experiments of dynein inhibition using genetic mutations on bidirectional axonal transport, have reported an overall decline in the motility of the cargo [7, 25, 42]. The mutual interplay of kinesin and dynein in activating each other during bidirectional transport was also studied through inhibition and depletion studies of peroxisome

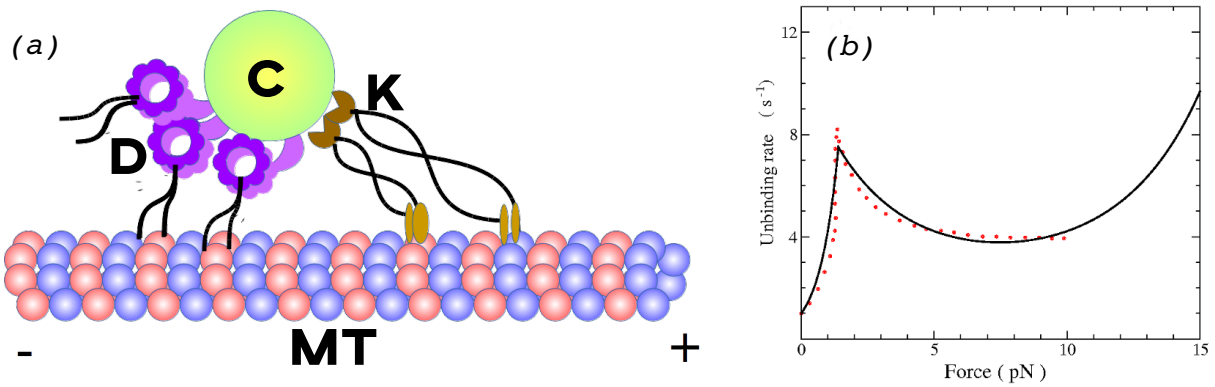

FIG. 1. (a) Schematic of bidirectional motion of cargo (C) attached to both kinesin (K) and dynein (D) motors on a microtubule (MT) filament; (b) Single dynein unbinding rate from experiments [29] (points) and the corresponding fit (solid line) from the TFBD model [58].

transport in *Drosophila melanogaster S2* cell [46]. It was observed that inhibition of kinesin motors abolishes transport towards the minus end and vice-versa. Similar results have been found in experiments involving dynein and dynactin mutations in *Drosophila* embryos [47]. Inhibition of dynein and dynactin produces severe impairment of plus end directed motion, providing further support for coordinated motion between the two motor species.

These apparently counterintuitive findings have been referred to as the *paradox of codependence*, suggesting some kind of coordination between the oppositely directed motors which has not been accounted for in the theoretical *tug-of-war* model [1, 25]. This invites the moot question on how the this paradox can be resolved and understood in terms of the underlying mechanism which governs bidirectional transport. In this work we seek to address this issue by re-examining the theoretical *tug-of-war* model [28, 30].

A striking difference between the single molecular behaviour of dynein and kinesin lies in their unbinding kinetics. Unlike kinesin, dynein can exhibit catchbonding, where the propensity for the dynein motors to unbind from cellular filament decreases when subjected to increased load force (Fig1b) [29, 54, 55]. *In-vivo* experiments on lipid droplets in drosophila embryos have measured the residence times - the time the cargo remains bound before detaching - of cargo driven by kinesin and dynein motors under superstall forces. While the residence time of kinesin decreases with increasing force, for dynein the behaviour is reversed and and the residence time is enhanced with increasing opposing load [55]. Similar *in-vitro* experiments with polystyrene beads carried by kinesins and cytoplasmic dynein have con-

firmed this atypical behaviour for dynein motors [29]. Further the distribution of residence times were used to extract a characteristic detachment time and hence dissociation rates as a function of force. These experiments unambiguously show that the detachment rate of dynein increases until the stall force, followed by a *catch bond* regime where the detachment rate decreases with increasing force. In contrast, the detachment rate of kinesin motors increases exponentially with increasing load force - a characteristic of *slip bond* [27, 55–57]. However this complex behaviour of detachment kinetics of dynein motors has not been taken into account in the *tug-of-war* theoretical description and instead the detachment rates for both dynein and kinesin motors from the MT filament are modeled as a simple exponentially increasing function of force [27, 28]. In our recent theoretical modeling work, accounting for catchbonding in single dynein, we have presented a Threshold Force Bond Deformation (TFBD) model to fit the experimentally observed unbinding rate of single dynein motor in constant load force (Fig. 1b) [29, 58]. Further we have illustrated that even for the case of *unidirectional transport* of cellular cargo by many dynein motors, the collective transport properties can be significantly affected by catchbonding behaviour [58].

In this paper, we focus our attention on this crucial ingredient of *catchbonding* that is exhibited by the dynein motors and which is missing in the previous theoretical formulation for describing bidirectional transport. We use the TFBD model for dynein, along with the usual slip bond model for kinesin [27, 28], to study the transport properties of bidirectional cargo motion. We use experimentally relevant measures to characterize the transport properties of cellular cargo : (i) average processivity, defined as the mean distance a cargo travels along a filament before detaching, and (ii) probability distributions of runtimes in the positive and negative directions and probability distributions of pause times. Using these measures we show that in an experimentally viable parameter space, catchbonding can indeed manifest itself in the transport properties of the cellular cargo exhibiting features consistent with experimental observations of mutual codependence of kinesin and dynein. Our model thus reproduces both the tug-of-war model transport characteristics and *codependent* transport characteristics in appropriate biological regimes.

Parameter	Symbol	Kinesin		Dynein	
Stall Force	$F_{s\pm}$	6 pN	[60]	1 pN (Weak dynein) 7 pN (Strong dynein)	[61] [62]
Detachment Force	$F_{d\pm}$	3 pN	[60]	0.67 pN	[29, 58]
Zero force attachment rate	$\pi_{0\pm}$	5/s	[63]	1/s	[64]
Zero force detachment rate	$\varepsilon_{0\pm}$	1/s	[60]	(0.1 - 10)/s	[65]
Deformation force scale	F_0	NA		7 pN	[29, 58]
Forward velocity	$v_{F\pm}$	$0.65\mu m/s$	[66]	$0.65\mu m/s$	[67]
Backward velocity	$v_{B\pm}$	$1nm/s$	[66]	$1nm/s$	[68, 69]

TABLE I. Single motor parameter values used in the simulations. The deformation force scale F_0 is a phenomenological parameter, as determined in Ref. [58]. The forward (or backward) velocities of kinesin and dynein are of comparable scales, and we have used the same value for both motors for simplicity.

RESULTS

We study transport of a cellular cargo with N_+ kinesin motors and N_- dynein motors. Each of these motors stochastically bind to a MT filament with rates $\pi_\pm$ and unbind from the filament with rates $\varepsilon_\pm$. The instantaneous state of the cargo is expressed in terms of the number of kinesin ($0 \leq n_+ \leq N_+$) and dynein ($0 \leq n_- \leq N_-$) motors that are attached to the filament. At any instant only the attached set of motors generate force on the cargo and are involved in its transport. For a set of similarly directed attached motors, we assume that the load force experienced by each motor is shared equally between them. We use the Stochastic Simulation Algorithm (SSA) [70, 71] to obtain individual cargo trajectories governed by the associated Master Equation (see Section Methods for details) for the probabilities in state space of attached kinesin and dynein. The cargo is considered to detach from the MT filament when no motors are attached ($n_+ = n_- = 0$). The simulated trajectories are then analysed to quantify the statistical properties of the system.

Detailed experimental studies have revealed that dynein motors exhibit catchbonding at forces larger than the stall force, F_{s-}, defined as the load force at which the cargo stalls (cargo velocity $v_c = 0$). This catchbonding regime is characterised by a decreasing detachment rate

with increasing opposing load. The unbinding rate of a single dynein is modeled by

$$\varepsilon_-(F) = \varepsilon_{0-} \exp\left(-E_d(F) + F/F_{d-}\right), \tag{1}$$

where the deformation energy E_d sets in beyond the stall force, and is modeled by a phenomenological equation [58],

$$E_d(F) = \Theta(F - F_{s-})\alpha \left[1 - \exp\left(-\frac{F - F_{s-}}{F_0}\right)\right], \tag{2}$$

The parameter α sets the strength of the catch bond, while F_{d-} and F_0 characterise the force scales for the dissociation energy and the deformation energy respectively. This correctly reproduces the experimentally reported dissociation dynamics of a single dynein as shown in Fig. 1(b) [58]. The unbinding kinetics of kinesin exhibits usual *slip* behavior (unbinding rate increasing exponentially with increasing load force). The characteristic stall forces and detachment forces of kinesin are denoted by F_{s+} and F_{d+} respectively. The values for the various parameter used in the stochastic simulations are listed in Table I.

The non-linear force response of the catch-bonded dynein has non-trivial implications for the transport properties of cargo during bidirectional transport. We investigate the consequences of this non-linear behaviour using the average processivity of the transported cargo and the probability distributions of cargo runtime and pausetimes in a particular direction. We relate it with the nature of individual cargo trajectories, observed in the context of various *in-vivo* and *in-vitro* experiments.

Processivity characteristics

In Fig. 2 (a) we look at the effect of variation of N_- on processivity, defined as the net displacement of the cargo until it unbinds. In the absence of catch bond ($\alpha = 0$), for a fixed value of N_+, the processivity decreases continuously with increasing N_- although staying positive throughout, indicating a decreasing net movement in the positive direction, as expected from the conventional tug-of-war argument. Within the range of parameters investigated in our model, the dynein stall force has no effect on the behavior. When catch bond is incorporated ($\alpha > 0$), the consequences are quite dramatic. For strong dynein ($F_{s-} = 7$pN), the processivity in the positive direction drops significantly even for one dynein motor, almost stalling the cargo. Increasing N_- further, eventually stalls the cargo, with

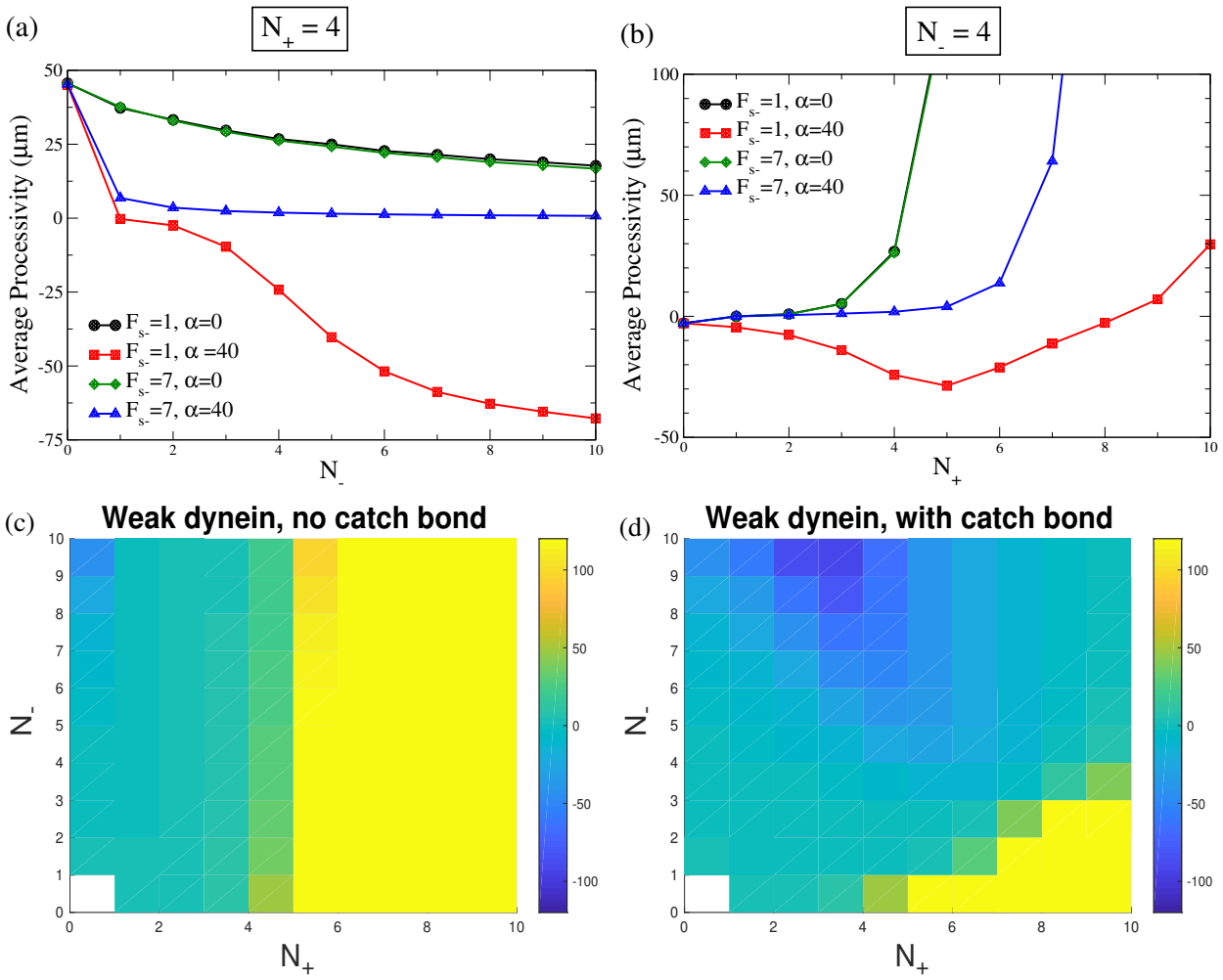

FIG. 2. Processivity (a) as a function of N_- for $N_+ = 4$, and (b) as a function of N_+ for $N_- = 4$. Contour plots for processivity in the $N_+ - N_-$ plane for (c) $F_{s-} = 1pN, \alpha = 0$, and (d) $F_{s-} = 1pN, \alpha = 40k_BT$. The colorbar indicates the average processivity (in μm). Yellow regions denote strong plus ended runs, while dark blue regions indicate strong minus ended runs. The zero-force (un)binding rates for dynein are $\varepsilon_{0-} = \pi_{0-} = 1/s$

no movement observed in either direction. For weak dynein ($F_{s-} = 1$pN), increasing N_- not only stalls the cargo, but also forces it to move in the negative direction. Weak dynein switches on its catchbond at smaller values of load force, leading to an increased propensity to latch on to the filament. This results in negative-end directed motion even for a small number of dynein motors. Strong dynein does not engage its catchbond until at relatively high values of load force. Although this helps lowering the processivity, it is not sufficient to pull it in the negative direction, therefore bringing it to a stall. This feature simultaneously

highlights the role of catchbonding in mediating codependent transport, including reversal of direction of cargo traffic, and the role of the stall forces of the dynein motors in determining transport behavior of cellular cargo.

In Fig. 2 (b), we look at the effect of variation of N_+ on processivity, for a fixed value of N_-. Without catch bond ($\alpha = 0$), increasing the maximum number of kinesin motors leads to a rapid increase of processivity in the positive direction due to the larger pull of the kinesin motors. Strong and weak dynein show the same characteristic features. In the presence of catch bond ($\alpha > 0$), strong dynein behaves qualitatively similarly to that without catch bond, although the movement in the positive direction occurs at a significantly higher N_+. Weak dynein on the other hand engages its catch bond even for small load forces and is therefore pulled further in the negative direction. This leads to the striking phenomenon of increasing negative directed motion on initially increasing the number of kinesin motors. Beyond a certain number of kinesins, the motion in the negative direction is hindered, and eventually, for very large N_+, the kinesin motors take over, leading to net positive-directed motion. This initial counter-intuitive increase of processivity in the negative direction is a remarkable feature of the effect of catch bond on bidirectional transport of cargo, where increasing the number of motors of one type facilitates motion in a direction opposite to that expected from usual tug-of-war arguments, and is reminiscent of the *paradox of codependence*.

The corresponding contour plots of the processivity of the cargo in the $(N_+ - N_-)$ plane are shown in Fig. 2(c-d), for weak dynein where the effect of dynein catch-bond is robust. As expected, in the absence of catch-bond ($\alpha = 0$) (Fig. 2(c)), there is a smooth transition at a critical N_+ from a regime where the cargo moves in the negative direction to one which moves in the positive direction. This critical N_+ is almost independent of N_- in accordance with our observation in Fig. 2(a-b). In the presence of catch-bonded dynein (Fig. 2(d)), we observe a distinct regime where the processivity increases in the negative direction on increasing N_+, the maximum number of kinesin motors. Further, for large N_-, the cargo is either in stall or moves in the negative direction as opposed to the behavior in the absence of dynein catch-bond. Plus-end directed motion occurs only in a small region of the (N_+, N_-) space for large N_+ and low N_-. The phase plot therefore provides an experimentally testable parameter space to explore the apparently anomalous codependent behavior observed in bidirectional transport when dynein catch bond is incorporated in the tug-of-war model. It is also possible to understand the effect of catch bond on processivity

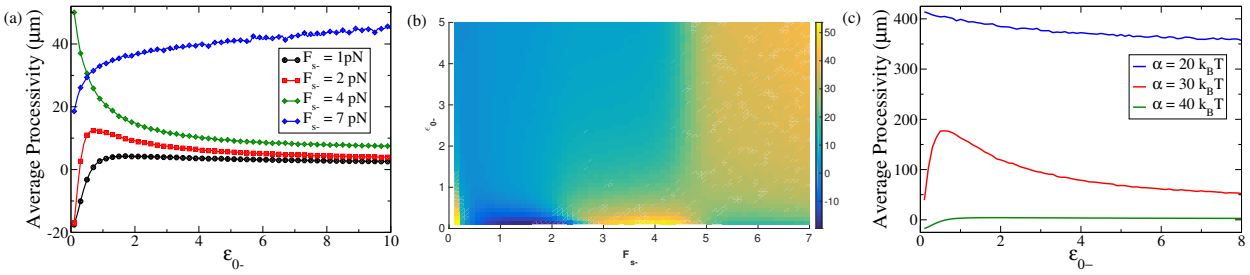

FIG. 3. (a) Processivity as a function of ε_{0-} for different stall forces at $\alpha = 40k_BT$; (b) Contour plots of processivity in $(F_{s-} - \varepsilon_{0-})$ plane for $\alpha = 40k_BT$; (c) Processivity as a function of ε_{0-} for different catch bond strengths (α) for weak dynein ($F_{s-} = 1pN$). Data shown is for $N_+ = 6$, $N_- = 2$, $\pi_{0-} = 1/s$

in terms of the average number of bound motors (see Supplementary Fig. S3 for details) which corroborate the features observed in Fig. 2.

Experimental techniques to modulate cargo processivity can also be achieved by modifying the binding/unbinding rates of the motor proteins. Dynactin mutations in *Drosophila* neurons affect the kinetics of dynein binding to the filament, leading to cargo stalls [42]. To investigate this, we tune the bare unbinding rate of dynein motor (ε_{0-}) with the dynein catch bond switched on (Fig. 3). For a fixed set of (N_+, N_-), we observe that for weak dynein ($F_{s-} = 1pN$ in Fig. 3(a)), the processivity starts to decrease from a negative value, as the bare unbinding rate is increased, as expected. However, beyond a critical ε_{0-}, the processivity saturates to a small positive value. Increasing ε_{0-} effectively weakens the propensity of dynein to stay attached to the filament. Beyond the critical ε_{0-}, weakening the dynein further does not lead to any increase in the run length in the positive direction, as might be expected from a conventional *tug-of-war* scenario, but rather the catch bond ensures that there is no change in the run length. At a slightly higher F_{s-}, ($F_{s-} = 2pN$ in Fig. 3(a)), on increasing ε_{0-}, the run length in the negative direction decreases, reaching a positive value. On increasing the unbinding rate further, the processivity in the positive direction decreases instead of increasing, eventually saturating to a positive value, highlighting the complex interdependence of interactions between kinesin and dynein arising completely due to the dynein catch bond. At a larger value of the stall force ($F_{s-} = 4pN$), on weakening dynein, the run length in the positive direction decreases, throughout the ε_{0-} range. This counterintuitive result again is purely due to catch bonding of dynein, giving rise to de-

creasing positive directed walks as the unbinding strength of minus motors is increased. For strong dynein ($F_{s-} = 7pN$), we recover back the expected trend of conventional tug-of-war models, where increasing the unbinding rate consistently increases the processivity in the positive direction.

This entire spectrum of behaviour can be visualised as a phase plot of the processivity in the ($F_{s-}-\varepsilon_{0-}$) plane (Fig. 3(b)). These contour plots captures the richness of the processivity behaviour due to catchbonding . For instance in Fig. 3(b) for a range of stall force for dynein F_{s-} between $1.5pN$ and $2.5pN$, effect of increase of ε_{0-} can result in initial decrease in minus-end runs, leading to net positive run length. Increasing ε_{0-} further, leads to a reduction of the positive run length due to catchbonding and a behaviour akin to reentrant behaviour [72] is observed. The phase plot also highlights the role of the tenacity of dynein motors in determining the overall motion of the cellular cargo. For example, for a fixed low value of $\varepsilon_{0-} < 0.5s^{-1}$, initially an increase in F_{s-} leads to rapid switch of the direction of net motion of a cargo from minus end directed motion to plus-end directed motion. Subsequently, an increase in F_{s-} leads to lower positive processivity. For $\varepsilon_{0-} > 0.5s^{-1}$, the motion of cargo shows monotonic increase in processivity with increasing F_{s-}.

The strength of catchbond also plays an important role in determining the nature of processivity of the cargo. In Fig. 3(c), we illustrate the variations in processivity on varying the catch bond strength for weak dynein. The catch bond strength can dramatically alter the processivity features. This is a phenomenological input in our model, and further experiments on the exact mechanism of the catch bond in dynein can help identify biologically relevant regimes for α and therefore constrain the predictions of the model.

These different processivity characteristics highlight the mediating role played by catchbonding in dynein in fashioning the overall motility behaviour of the cellular cargo. Accounting for catch bonding of dynein in the single vesicle transport model reproduces the whole range of observed experimental features, from conventional *tug-of-war* models to codependent transport depending on the appropriate parameter regimes and provides a resolution of the *paradox of codependence*. It also highlights that not only does the catch bonding of dynein result in whole gamut complex motility behaviour of cellular cargo, but it serves the role of potential control point in determining and regulating motor driven intracellular transport.

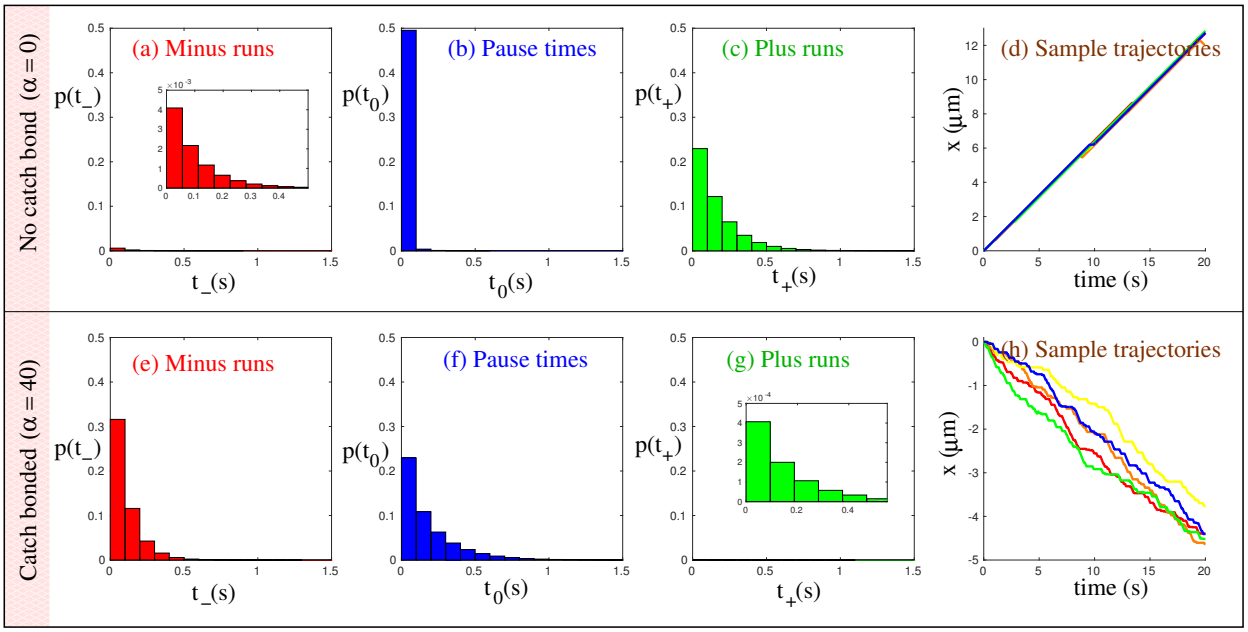

FIG. 4. Probability distributions of runtimes for $N_+ = 2$, $N_- = 6$. The top panel shows the normalized histograms and sample trajectories for dynein in the absence of catch bond ($\alpha = 0$). The bottom panel shows the corresponding quantities for catch-bonded dynein ($\alpha = 40$). (a) and (e) Distributions of runtimes for minus directed runs (shown in red); (b) and (f) pausetime distributions (shown in blue); (c) and (g) distributions of runtimes for minus directed runs (shown in green); and (d) and (h) sample trajectories. Insets, where present, show a magnified view of the probability distributions.

Probability Distribution of run and pause times

Experiments on *in-vitro* and *in-vivo* systems of endosome motion have established that there is often an asymmetry in the number of motors that are simultaneously attached to a cargo. To check whether our model can account for the experimental observations, we focus on two distinct cases of endosome transport where there are experimental estimates for the number of motors attached to the cargo. The role of catchbonding in determining the specific nature of bidirectional transport and corresponding cellular cargo trajectories can be understood by analyzing the the probability distributions of the time the cargo spends in the paused (*tug-of-war*) state versus the time it spends in the moving plus-end directed and minus-end directed state.

In *dictyostelium* cell extracts, it has been reported that teams of four to eight dyneins and

one to two kinesins are simultaneously attached to a cargo [38]. The resultant motion was observed to be minus-end directed with intermittent pauses. To understand these results in the context of our model, we fixed $N_+ = 2$ and $N_- = 6$ (Fig. 4). In the absence of catchbonding, the resultant motion is strongly plus-end directed, as can be seen from the trajectory plots in Fig. 4(d). The probability distributions of runtimes show that there are many more kinesin runs (Fig. 4(c)) than dynein runs (Fig. 4(a)), and the average runtime is also higher in the case of kinesins. The pauses in this case are also of extremely short duration (Fig. 4(b)), leading to strongly plus-end directed runs. As an aside we also note that the overall frequency of the cargo in the pause phase always adds up to 0.5 and similarly the overall frequency of the combined positive and negative run adds up to 0.5. This is simply a consequence of the conservation of probability. Due to the stall force of kinesin motor being about 5 times that of dynein and the bare binding rate of kinesin being larger than dynein (see Table I), even with $N_+ < N_-$, a plus-end directed run, on average, continues for a longer time than a minus-end directed run, leading to larger average runtimes along the positive direction. When dynein catch bond is switched on, the picture changes dramatically. Minus-ended runs become much more frequent than plus-ended runs, while the average pause time also increases by an order of magnitude compared to the non-catchbonded case, and becomes comparable to the average minus directed runtimes. This is shown in Figs. 4(e)-(g). Load force on dynein due to attached kinesin engages the catch-bond, making it more difficult to unbind from the filament. Therefore, we see that the manifestation of catchbonding in dynein results in strong minus directed runs with longer duration pauses, as is shown in Fig. 4(h). This qualitatively agrees with the experimental observation of transport of endosomes in *Dictyostelium* cells [38].

In a separate set of experiments which looks at bidirectional motility behaviour of early endosomes in fungus *Ustilago maydis*, it has been seen that a team many kinesin motors (3-10) are involved in *tug-of-war* with only 1 or 2 dynein motors during transport [15]. To study the ramification of catchbond in such a scenario wherein several kinesin motors are in opposition to very few dynein motors, we generate the probability distribution of pause times along with minus-end and plus-end directed runtimes for a cargo being transported by 6 kinesins and 2 dyneins ($N_+ = 6, N_- = 2$). The results displayed in Fig. 5 illustrates that while in the absence of catchbonding in dynein, the resultant motion would be strongly plus-end directed, with very small pause times, incorporation of catchbonding in dynein affects

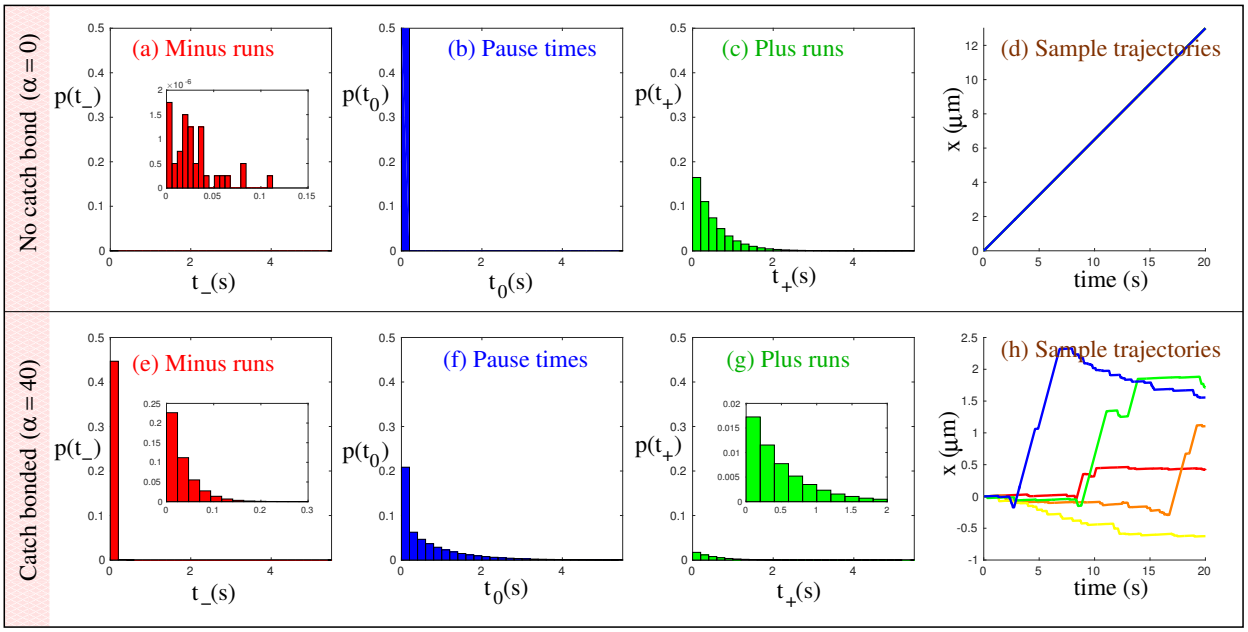

FIG. 5. Probability distributions of runtimes for $N_+ = 6$, $N_- = 2$. The top panel shows the normalized histograms and sample trajectories for dynein in the absence of catch bond ($\alpha = 0$). The bottom panel shows the corresponding quantities for catch-bonded dynein ($\alpha = 40$). (a) and (e) Distributions of runtimes for minus directed runs (shown in red); (b) and (f) pausetime distributions (shown in blue); (c) and (g) distributions of runtimes for minus directed runs (shown in green); and (d) and (h) sample trajectories. Insets, where present, show a magnified view of the probability distributions.

the probability distribution in a manner wherein, the frequency of minus-ended runs exceeds the frequency of plus-ended runs by almost one order of magnitude. However, the average duration of the minus-ended runs is about one order of magnitude lower than that of the plus-end directed run duration. Further the effect of catchbond leads to significant substantial duration of pauses ($1 - 4sec$) during transport. These characteristics of the probability distributions result in typical cargo trajectories which exhibits bidirectional motion with pauses.

Motility diagrams and processivity

An important tool in the theoretical analysis of cellular transport by molecular motors has been through the use of motility diagrams, which characterize the phase space in terms

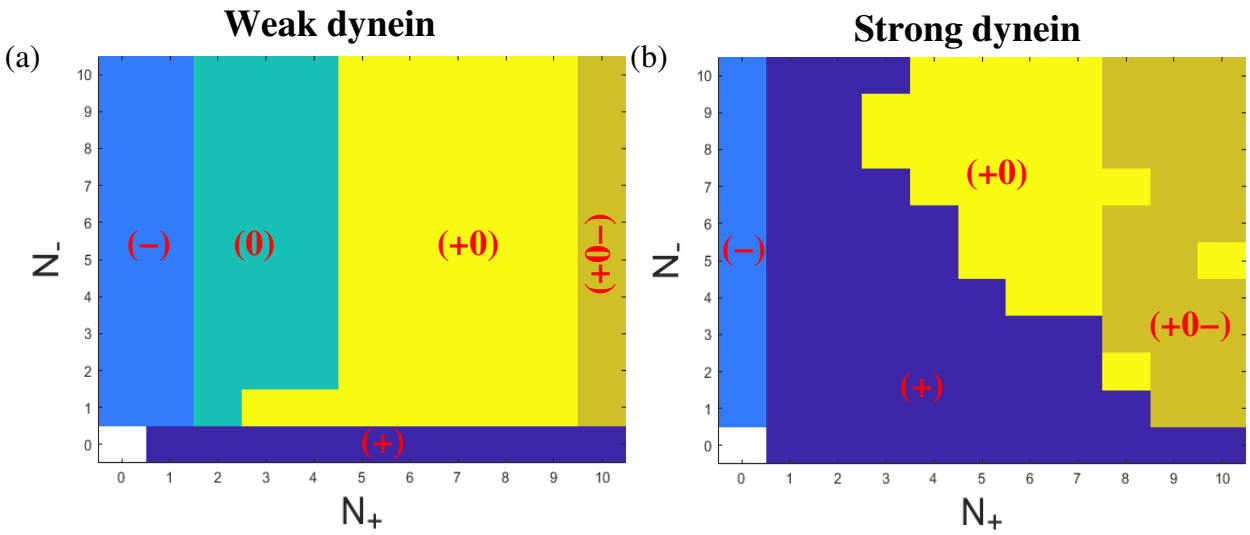

FIG. 6. Motility diagrams in the $N_+ - N_-$ plane for (a) Weak dynein ($F_{s-} = 1pN$), and (b) Strong dynein ($F_{s-} = 7pN$). There are seven possible motility states, *fast plus* (+), *fast minus* (-), *no motion* (0), *fast plus with pauses* (0+), *fast minus with pauses* (0-), *fast bidirectional motion* (+-), and *fast bidirectional with pauses* (-0+). The parameter values used are the same as in Fig. 2.

of the peaks of the steady state probability distribution of attached motors. A peak in the probability distribution at $(n_+^*, 0)$ corresponds to plus directed motion, while a peak at $(0, n_-^*)$ corresponds to minus-directed motion, and a peak at $(n_+^* \neq 0, n_-^* \neq 0)$ corresponds to a paused or tug-of-war state. If there is a single peak in the probability landscape, then the net motion can be of three types, *fast plus* (+), *fast minus* (-) or *no motion* (0). Multiple peaks are also possible and introduce four more possible types of motion, *fast plus with pauses* (0+), *fast minus with pauses* (0-), *fast bidirectional motion* (+-), and *fast bidirectional with pauses* (-0+). The motion is then categorised into one of these seven classes depending on the number and nature of peaks of the probability distribution.

However, the motility diagram approach has some inherent limitations since interpreting the motion in terms of the peaks may give an incomplete picture when the number of attached motors is very few, as is the case considered here. In Fig. 6, we plot the motility diagram for $\alpha = 40k_BT$ and $\epsilon_{0-} = \pi_{0-} = 1/s$ for $F_{s-} = 1pN$ and $F_{s-} = 7pN$. We can compare these plots with the contour plots of the processivity obtained for these same parameters as shown in Fig. 2 (d) and Fig. S2 (b). As can be seen clearly, the motility diagrams do not capture the full complexity of motion in the presence of catch bonds. For

weak dynein, the motility diagrams predict that for $N_+ > 1$ and $N_- > 2$, the motion is either paused or in the fast plus with pause state. However, as the processivity contour plots make clear, there is a range of (N_+, N_-) where the nonlinear effects of the dynein unbinding rate actually result in negative directed runs in this region. This can also be seen by considering the runtime probability distributions shown in Figs. 4 and 5. For example for $N_+ = 2$ and $N_- = 6$, we have a minus directed transport interspersed with pauses, while the motility diagram simply predicts a no-motion state. Thus for the characterisation of transport characteristics in these low attached motor regimes, the use of processivity contour plots and runtime probability distributions as illustrated in this paper provide a more accurate approach than the conventional motility diagrams.

DISCUSSION

The paradox of codependent transport [25] is in direct contradiction to the standard mechanical tug-of-war [15, 28, 30] picture between kinesins and dyneins. In particular it has been experimentally observed that inhibiting the activity of one type of motor can actually lead to an overall decline of motility of the cellular cargo being transported by oppositely directed set of motor proteins. A missing ingredient from existing theoretical models has been the catchbonding behaviour of dyneins, where the unbinding rate of dyneins shows a non-monotonic dependence on opposing loads [29, 38].

In this article we have explicitly shown how incorporation of catchbonding behaviour of dynein motors in the modeling approach for bidirectional transport is able to resolve this paradox and provide a coherent picture of apparently disparate set of experimental observations. Many of the *in-vivo* and *in-vitro* experiments have characterized the nature of bidirectional transport in terms of cargo particle trajectories [15, 38]. Applying our model which includes the effect of catchbond in dynein, qualitatively reproduces the experimentally observed features of cargo trajectories during transport. We also find that the processivity characteristics of the cargo need not be in sync with the theoretical construct of *motility diagrams* [28, 30] as illustrated by comparison of Fig.2 with Fig.7. Thus the findings of our model points to the crucial role played by catchbonding in dynein motors in bidirectional transport, highlighting its significance as an internal regulatory mechanism during transport, *albeit through mechanical interaction between the motors*. We specifically summarize some

of the key experiments below and how the experimental observations tie in with predictions of our catchbond model.

The effect of dynein motor inhibition on bidirectional transport was studied in *Drosophila* neurons through mutations in the dynein heavy chain (cDHC) and in the dynactin complex [42]. The heavy chain mutations in dynein inactivate the dynein motors and hence in the framework of our theory, corresponds to the decrease in the number of dyneins that can bind to the cargo. This can then be modeled through a decrease in the dynein number N_-. The mutation in the dynactin complex, on the other hand, affects the chemical kinetics of the binding-unbinding process of the dynein motor to the MT filament. Within our framework, we model this effect through varying the zero force unbinding rate of dynein, ε_{0-}. While both decreasing N_- or increasing ε_{0-} has the effect of weakening the dynein motor action, the manifestation of these two effects in the transport characteristics can in general be distinct. The results of these experiments can then be understood in the light of Figs. 2(a) and 3(a), where a decrease in N_-, or an increase in ε_{0-} can, for appropriate stall forces, reduce the average processivity to zero, corresponding to stalled motion of the cargo.

Diverse experiments have also indicated that mutations of conventional kinesin in Drosophila can hamper motion of cellular cargo in both directions [73–75]. This is consistent with the results shown in Figs. 2(b), where reducing the kinesin number can stall cargo motion completely. Interestingly, while kinesin exhibits a conventional slip bond, the cooperative force exerted by the catch bonded dynein on kinesins, and vice versa, introduce a complex interplay which results in signatures of codependent transport being observed even on varying effective kinesin numbers. For example, as shown in Fig. 2(b) for weak dynein, reducing the number of kinesin, can in certain ranges, decrease the overall motion of the cargo in the negative direction. This counterintuitive phenomenon is a direct manifestation of the dynein catch bond, through the nonlinear unbinding kinetics of dynein motors. Similar results pointing to codependent regulation of bidirectional transport has been seen in studies of peroxisome transport in *Drosophila melanogaster S2* cell [46], as well as in *Drosophila* embryos [47]. Our tug-of-our picture then, with the introduction a mechanical regulation mediated by the dynein catch bond, presents a unified resolution of the experimental observations of codependent transport through mutations of both kinesin and dynein motor proteins. Curiously enough, these processivity characteristics also point to the sharp difference in transport characteristics of dynein with high tenacity when com-

pared to weak tenacity. In the former case regulatory role of catchbonding is very weak since the typical force scale at which catchbond is activated is quite high with respect to the typical load forces experienced by the motors. It would indeed be interesting to probe further if this is the reason for the *strong* dynein in yeast not being involved in transport, while *weak* mammalian dynein are crucial to intracellular transport.

Many of the *in-vivo* and *in-vitro* experiments have characterized the nature of bidirectional transport in terms of cargo particle trajectories. Experiments on different systems have reported different number of average bound kinesins and dyneins. For instance for experiments on endosome motion in *Dictyostelium* cell [38] have reported that 1-2 kinesin are opposed by teams of 4-8 dyneins, and the resultant cargo trajectories are minus-end directed. On the other hand for endosome motion for *Ustilago maydis*, it has been observed that typically one or two dyneins oppose teams of four to six kinesins, and the resultant trajectories showed bidirectional motion [15]. In order to test the consistency of our theoretical picture with the observed set of experimental trajectories of the transported cargo we obtain the probability distribution of runtimes for plus-ended and minus-ended runs and the pause time distributions for our simulated cargo trajectories (Figs. 4 and 5), using the typical motor parameters of kinesin and dynein. Remarkably, we find that the incorporation of catchbonding in dynein qualitatively reproduces the experimentally observed features of transport. In the absence of catchbonding, the conventional tug-of-war stochastic model predicts positive-directed trajectories in these regimes, and only the nonlinear unbinding response of catch bonded dynein can explain the observed experimental trajectories.

While our phenomenological model has successfully been able to qualitatively capture many of the aspects of motor driven bidirectional cargo transport, for a more quantitatively accurate and comprehensive analysis of the transport the theory needs to be refined to take in account many of the other experimental observations. First of all, some experiments have pointed to the presence of external regulatory mechanism which coordinates the action of the motors and the resultant transport of the cargo [1, 8, 47, 76–82]. For instance, it has been observed that the transport of lipid droplets in *Drosophila* is regulated by *Klar* protein [1, 8]. In the absence of *Klar* protein transport of the droplets is severely disrupted although the motor functionality is not affected suggesting its regulatory role [1, 8]. Some recent experiments have also suggested that other factors such as the interactions between multiple motors leading to clustering, and the rotational diffusion of the cargo itself can play a role

in the regulatory mechanism [83, 84]. Thus it requires a careful examination of the various experiments to delineate the relative importance of mechanical regulation that is mediated through catchbonding in motors and the external modes of regulating transport. Secondly, one simplification that has been made in our phenomenological model is the assumption of equal load sharing by the motors. However it has been experimentally observed that load is not shared equally between all dynein motors, rather the leading motor of a team of attached motors bears a larger part of the load, which is also demonstrated by bunching of motors at one end [54, 85]. Further for dynein motors it has been observed that under load, dynein has a variable step size. For forces below the stall force, dynein modulates its step-size from $24nm$ for zero load forces to 8nm for forces close to the stall force [69, 86, 87]. Beyond the stall force, the catch bond activates reducing the dynein dissociation rate [29, 86]. The aspect of variable step size has not be taken into consideration in our theoretical description.

In summary, our phenomenological model illustrates the key principle that the incorporation of a dynein catch bond can provide a mechanical explanation of the phenomenon of codependent transport by teams of opposing molecular motors. The model is able to capture the broad qualitative features observed in context of a multitude of experiments on motor driven transport within the cell. The framework proposed here encapsulates both the tug-of-war and codependent behaviour in appropriate regimes and hence provides an unifying picture of motor-driven transport.

METHODS

A. Model

At any instant of time, the state of the cargo is characterised by the number of attached Kinesin (n_+)and Dynein motors (n_-). The maximum of number of kinesin and dynein motors are N_+ and N_- respectively ($0 < n_+ < N_+$ and $0 < n_- < N_-$). The time evolution of the system is then governed by the master equation [28]

$$\begin{aligned}\frac{\partial p(n_+,n_-)}{\partial t} &= p(n_+ + 1, n_-)\epsilon_+(n_+ + 1, n_-) + p(n_+, n_- + 1)\epsilon_-(n_+, n_- + 1) \\ &+ p(n_+ - 1, n_-)\pi_+(n_+ - 1, n_-) + p(n_+, n_- + 1)\pi_+(n_+, n_- + 1) \\ &- p(n_+, n_-)\left[\epsilon_+(n_+, n_-) + \epsilon_-(n_+, n_-) + \pi_+(n_+, n_-) + \pi_-(n_+, n_-)\right] \end{aligned} \tag{3}$$

where, $p(n_+, n_-)$ is the probability to find the cargo with n_+ kinesin and n_- dynein motors.

The kinesin and dynein binding rates are assumed to be of the form

$$\pi_\pm = (N_\pm - n_\pm)\pi_{0\pm} \tag{4}$$

where $N_+\pi_{0+}$ ($N_-\pi_{0-}$) is the rate for the first kinesin (dynein) motor to bind to the MT.

The unbinding rate for kinesin is given by the expression

$$\varepsilon_+(n_+, n_-) = n_+\varepsilon_{0+} \exp[F_c(n_+, n_-)/(n_+F_{d+})] \tag{5}$$

while the unbinding rate for dynein is given by

$$\varepsilon_-(n_+, n_-) = n_-\varepsilon_{0-} \exp[-E_d(F_c(n_+, n_-)) + F_c(n_+, n_-)/(n_-F_{d-})] \tag{6}$$

with the catch bond deformation energy given by

$$E_d(F_c(n_+, n_-)) = \Theta(F_c(n_+, n_-)/n_- - F_{s-})\alpha\left[1 - \exp\left(-\frac{F_c(n_+, n_-)/n_- - F_{s-}}{F_0}\right)\right] \tag{7}$$

Here, $\varepsilon_{0\pm}$ denotes the zero-force single motor unbinding rates, while α parameterizes the strength of the catch bond. The cooperative force felt by the motors due to the effect of the motors of the other species is given by [30]

$$F_c(n_+, n_-) = \frac{n_+n_-F_{s+}F_{s-}}{n_-F_{s-}v_{0+} + n_-F_{s-}v_{0+}}(v_{0+} + v_{0-}) \tag{8}$$

and the cargo velocity is given by

$$v_c(n_+, n_-) = \frac{n_+F_{s+} - n_-F_{s-}}{n_-F_{s-}/v_{0-} + n_+F_{s+}/v_{0+}} \tag{9}$$

Here, $v_{0\pm}$ denotes the velocity of kinesin (or dynein) motors,

$$v_{0+} = \begin{cases} v_{F+} \;\; if \;\; v_c > 0 \\ v_{B+} \;\; if \;\; v_c < 0 \end{cases} \quad \text{and} \quad v_{0-} = \begin{cases} v_{F-} \;\; if \;\; v_c < 0 \\ v_{B-} \;\; if \;\; v_c > 0 \end{cases} \tag{10}$$

where, v_F and v_B are the forward and backward motor velocities. Finally the stall forces for the two motor species are denoted by $F_{s\pm}$.

The parameters used in the study are taken from the literature, and are summarized in Table I.

B. Numerical techniques

The time trajectory of the cargo is obtained by simulation the master equation using Gillespie's Stochastic Simulation Algorithm (SSA) [70, 71]. All possible initial configurations were generated for a given (N_+, N_-) pair, and 1000 trajectories were evolved for each initial configuration. A run finishes if the simulation continues until the maximum time T_{MAX} or if all motors (both positive and negative) detach from the MT. The runlength was then averaged over all initial configurations and all iterations. Steady state probability distributions were also computed from the SSA trajectories after discarding initial transients.

The steady state probability distributions, and hence the motility diagrams, were also obtained by constructing the nullspace of the associated transfer matrix for the master equation. The probability distributions computed using the matrix method and the SSA algorithm matches exactly.

ACKNOWLEDGMENTS

MKM acknowledges financial support from the Ramanujan Fellowship (13DST052), Department of Science and Technology (DST), India and the IRCC Seed Grant, IIT Bombay (14IRCCSG009). AC acknowledges SERB project No. EMR/2014/000791 for financial support. NG, SC and AC thank the HPC facility at IISER Mohali for computational time. SC and AC acknowledges DST, India for financial support. The authors would also like to thank the organizers of the SMYIM conference, Goa, and the ISPCM conference, Bangalore, where part of this work was done. MKM would like to acknowledge the hospitality of MPIPKS,

Dresden, where part of this work was done. The authors would also like to acknowledge helpful discussions with Roop Mallik, TIFR.

---

[1] Welte, M. A. Bidirectional transport along microtubules *Curr.Biol.* **14**, R525-R537 (2004)

[2] McLaughlin, R. T., Diehl, M. R. and Kolomeisky, A. B. Collective dynamics of processive cytoskeletal motors. *Soft Matter* **12**, 14 (2016)

[3] Rebhun, L. I. Polarized intracellular particle transport: saltatory movements and cytoplasmic streaming. *Int. Rev. Cytol.* **32**, 93137 (1972)

[4] Rebhun, L.I. Structural aspects of saltatory particle movement. *J. Gen. Physiol.* **50** (Suppl), 223239 (1967)

[5] Hamm-Alvarez, S.F., Kim, P.Y., and Sheetz, M.P. Regulation of vesicle transport in CV-1 cells and extracts. *J. Cell Sci.* **106**, 955966 (1993)

[6] Rodionov, V., Yi, J., Kashina, A., Oladipo, A., and Gross, S.P. Switching between microtubule- and actin-based transport systems in melanophores is controlled by cAMP levels. *Curr. Biol.* **13**, 18371847 (2003)

[7] Gross, S.P., Tuma, M.C., Deacon, S.W., Serpinskaya, A.S., Reilein, A.R., and Gelfand, V.I. Interactions and regulation of molecular motors in Xenopus melanophores. *J. Cell Biol.* **156**, 855865 (2002)

[8] Welte, M.A., Gross, S.P., Postner, M., Block, S.M., and Wieschaus, E.F. Developmental regulation of vesicle transport in Drosophila embryos: forces and kinetics. *Cell* **92**, 547557 (1998)

[9] Suomalainen, M., Nakano, M.Y., Keller, S., Boucke, K., Stidwill, R.P., and Greber, U.F. Microtubule-dependent plus- and minus end-directed motilities are competing processes for nuclear targeting of adenovirus. *J. Cell Biol.* **144**, 657672 (1999)

[10] Smith, G.A., Gross, S.P., and Enquist, L.W. Herpesviruses use bidirectional fast-axonal transport to spread in sensory neurons. *Proc. Natl. Acad. Sci. USA* **98**, 34663470 (2001)

[11] Hollenbeck, P.J. The pattern and mechanism of mitochondrial transport in axons. *Front. Biosci.* **1**, d91d102 (1996)

[12] Ananthanarayanan, V., Schattat, M., Vogel, S. K., Krull, A., Pavin, N. and Tolić-Nørrelykke, I. M. Dynein Motion Switches from Diffusive to Directed upon Cortical Anchoring. *Cell* **153**,

1526-1536 (2013)

[13] Pavin, N. and Tolić-Nørrelykke, I. M. Dynein, microtubule and cargo: a mnage trois. *Biochem Soc. Trans.* **41**, 1731-1735 (2013)

[14] Rogers, S. L., Tint. I. S., Fanapour, P.C. & Gelfand, V. I. Regulated Bidirectional motility of melanophore pigment granules along microtubules *in vitro*. *Proc. Natl. Acad. Sci.* **94**, 3720-3725 (1997).

[15] Schuster, M., Lipowsky, R,, Assmann, M-A., Lenz, P. & Steinberg, G. Transient binding of dynein controls bidirectional long-range motility of early endosomes. *Proc. Natl. Acad. Sci.* **108**, 3618-3623 (2011)

[16] Chada, S.R., and Hollenbeck, P.J. Mitochondrial movement and positioning in axons: the role of growth factor signaling. *J. Exp. Biol.* **206**, 19851992 (2003)

[17] Murray, J.W., Bananis, E., and Wolkoff, A.W. Reconstitution of ATP-dependent movement of endocytic vesicles along microtubules in vitro: an oscillatory bidirectional process. *Mol. Biol. Cell* **11**, 419433 (2000)

[18] Valetti, C., Wetzel, D.M., Schrader, M., Hasbani, M.J., Gill, S.R., Kreis, T.E., and Schroer, T.A. Role of dynactin in endocytic traffic: effects of dynamitin overexpression and colocalization with CLIP-170. *Mol. Biol. Cell* **10**, 41074120 (1999)

[19] Hollenbeck, P.J. Products of endocytosis and autophagy are retrieved from axons by regulated retrograde organelle transport. *J. Cell Biol.* **121**, 305315 (1993)

[20] Blocker, A., Severin, F.F., Burkhardt, J.K., Bingham, J.B., Yu, H., Olivo, J.C., Schroer, T.A., Hyman, A.A., and Griffiths, G. Molecular requirements for bi-directional movement of phagosomes along microtubules. *J. Cell Biol.* **137**, 113129 (1997)

[21] Wacker, I., Kaether, C., Kromer, A., Migala, A., Almers, W., and Gerdes, H.H. Microtubule-dependent transport of secretory vesicles visualized in real time with a GFP-tagged secretory protein. *J. Cell Sci.* **110**, 14531463 (1997)

[22] Hayden, J.H. Microtubule-associated organelle and vesicle transport in fibroblasts. *Cell Motil. Cytoskeleton* **10**, 255262 (1988)

[23] Manneville, J.B., Etienne-Manneville, S., Skehel, P., Carter, T., Ogden, D., and Ferenczi, M. Interaction of the actin cytoskeleton with microtubules regulates secretory organelle movement near the plasma membrane in human endothelial cells. *J. Cell Sci.* **116**, 39273938 (2003)

[24] McDonald, D., Vodicka, M.A., Lucero, G., Svitkina, T.M., Borisy, G.G., Emerman, M., and Hope, T.J. Visualization of the intracellular behavior of HIV in living cells. *J. Cell Biol.* **159**, 441452 (2002)

[25] Hancock, W. O. Bidirectional cargo transport moving beyond tug of war. *Nature. Rev. Cell. Biol.* **15**, 615-626 (2014)

[26] Posta, F., D'Orsogna, M. R. and Chou, T. Enhancement of cargo processivity by cooperating molecular motors. *Phys. Chem. Chem. Phys.* **11**, 4851-4860 (2009)

[27] Klumpp, S. & Lipowsky, R. Cooperative cargo transport by several molecular motors. *Proc. Natl. Acad. Sci.* **102**, 17284-17829 (2005)

[28] Muller, M. J. I., Klumpp, S. & Lipowsky, R. Tug-of-war as a cooperative mechanism for bidirectional cargo transport by molecular motors. *Proc. Natl. Acad. Sci.* **105**, 4609-4614 (2008)

[29] Kunwar. A. *et. al*, Mechanical stochastic tug-of-war models cannot explain bidirectional lipid-droplet transport *Proc. Natl. Acad. Sci.* **108**, 18960-18965 (2011)

[30] Muller, M. J. I., Klumpp, S. & Lipowsky, R. Motility states of molecular motors engaged in a stochastic tug-of-war. *J. Stat. Phys.* **133**, 1059-1081 (2008)

[31] Mller, M. J., Klumpp, S. and Lipowsky, R. Bidirectional transport by molecular motors: enhanced processivity and response to external forces. *Biophys. J.* **98**, 26102618 (2010)

[32] Hendricks, A. G., Perlson E., Ross, J. L., Schroeder, H. W., Tokito, M., and Holzbaur, E. L. F. Motor coordination via a tug-of-war mechanism drives bidirectional vesicle transport. *Curr. Biol.* **20**, 697702 (2010)

[33] Yi, J. Y. et al. High-resolution imaging reveals indirect coordination of opposite motors and a role for LIS1 in high-load axonal transport. *J. Cell Biol.* **195**, 193201 (2011)

[34] Blehm, B. H., Schroer, T. A., Trybus, K. M., Chemla, Y. R. and Selvin, P. R. In vivo optical trapping indicates kinesins stall force is reduced by dynein during intracellular transport. *Proc. Natl Acad. Sci. USA* **110**, 33813386 (2013)

[35] Kapitein, L. C., Schlager M. A., van der Zwan, W. A., Wulf, P. S., Keijzer, N. and Hoogenraad, C. C. Probing intracellular motor protein activity using an inducible cargo trafficking assay. *Biophys. J.* **99**, 21432152 (2010)

[36] Caviston, J. P., Zajac, A. L., Tokito, M. and Holzbaur, E. L. Huntingtin coordinates the dynein- mediated dynamic positioning of endosomes and lysosomes. *Mol. Biol. Cell* **22**, 478492

(2011)

[37] Gennerich, A. and Schild, D. Finite-particle tracking reveals submicroscopic-size changes of mitochondria during transport in mitral cell dendrites. *Phys. Biol.* **3**, 4553 (2006)

[38] Soppina, V., Rai, A.K., Ramaiya, A. J., Barak, P. & Mallik, R. Tug-of-war between dissimilar teams of microtubule motors regulates transport and fission of endosomes. *Proc. Natl. Acad. Sci.* **106**, 19381-19386 (2009)

[39] Goldberg, D. J. Microinjection into an identified axon to study the mechanism of fast axonal transport. *Proc. Natl Acad. Sci. USA* **79**, 48184822 (1982)

[40] Brady, S. T. and Pfister, K. K. Kinesin interactions with membrane bounded organelles in vivo and in vitro. *J. Cell Sci. Suppl.* **14**, 103108 (1991)

[41] Waterman-Storer, C. M., Karki, S.B., Kuznetsov, S. A., Tabb, J. S., Weiss, D. G., Langford, G. M. and Holzbaur, E. L. F. The interaction between cytoplasmic dynein and dynactin is required for fast axonal transport. *Proc. Natl Acad. Sci. USA* **94**, 1218012185 (1997)

[42] Martin, M. A., Iyadurai, S. J., Gassman, A., Gindhart, J. G., Hays, T. S. and Saxton, W. M. Cytoplasmic dynein, the dynactin complex, and kinesin are interdependent and essential for fast axonal transport *Mol. Biol. Cell* **10**, 3717-3728 (1999)

[43] Encalada, S. E., Szpankowski, L., Xia, C. H. and Goldstein, L. S. Stable kinesin and dynein assemblies drive the axonal transport of mammalian prion protein vesicles. *Cell* **144**, 551565 (2011)

[44] Moughamian, A. J. and Holzbaur, E. L. Dynactin is required for transport initiation from the distal axon. *Neuron* **74**, 331343 (2012)

[45] Haghnia, M., Cavalli, V., Shah, S. B., Schimmelpfeng, K., Brusch, R., Yang, G., Herrera, C., Pilling, A. and Goldstein, S. B. Dynactin is required for coordinated bidirectional motility, but not for dynein membrane attachment. *Mol. Biol. Cell* **18**, 20812089 (2007)

[46] Ally, S., Larson, A. G., Barlan, K., Rice, S. E. & Gelfand, V. I. Opposite-polarity motors activate one another to trigger cargo transport in live cells. *J. Cell Biol.* **187**, 1071-1082 (2009)

[47] Gross, S. P., Welte, M. A., Block, S. M. and Wieschaus, E. F. Coordination of opposite-polarity microtubule motors. *J. Cell Biol.* **156**, 715 (2002)

[48] Deacon, S. W., Serpinskaya, A. S., Vaughan, P. S., Fanarraga, M. L., Vernos, I., Vaughan, K. T. and Gelfand, V. I. Dynactin is required for bidirectional organelle transport. *J. Cell Biol.*

160, 297301 (2003)

[49] Saxton, W. M. and Hollenbeck, P. J. The axonal transport of mitochondria. *J. Cell Sci.* **125**, 20952104 (2012)

[50] Pilling, A. D., Horiuchi, D., Lively, C. M. and Saxton, W. M. Kinesin-1 and Dynein are the primary motors for fast transport of mitochondria in Drosophila motor axons. *Mol. Biol. Cell* **17**, 20572068 (2006)

[51] Wang, X. and Schwarz, T. L. The mechanism of Ca^{2+}-dependent regulation of kinesin-mediated mitochondrial motility. *Cell* **136**, 163174 (2009)

[52] Uchida, A., Alami, N. H. and Brown, A. Tight functional coupling of kinesin-1A and dynein motors in the bidirectional transport of neurofilaments. *Mol. Biol. Cell* **20**, 49975006 (2009)

[53] Ling, S. C., Fahrner, P. S., Greenough, W. T. and Gelfand, V. I. Transport of Drosophila fragile X mental retardation protein-containing ribonucleoprotein granules by kinesin-1 and cytoplasmic dynein. *Proc. Natl Acad. Sci. USA* **101**, 1742817433 (2004)

[54] Mallik, R., Rai, A. K., Barak, P., Rai, A. & Kunwar, A. Teamwork in microtubule motors. *Trends in Cell Biol.* **23**, 575-582 (2013)

[55] Leidel, C., Longoria, R. A., Gutierrez, F. M. & Shubeita, G. T. *Biophys. J* **103** 492 (2012)

[56] Prezhdo, O. V. and Pereverzev, Y. V. *Phys. Rev. E* **73**, 050902 (2006).

[57] Mikhailenko, S. V., Oguchi, Y. and Ishiwata, S. Insights into the mechanisms of myosin and kinesin molecular motors from the single-molecule unbinding force measurements. *J. R. Soc. Interface* **7**, S295-S306 (2010)

[58] Nair, A., Chandel, S., Mitra, M., Muhuri, S. & Chaudhuri, A. Effect of catch bonding on transport of cellular cargo by dynein motors. *Phys. Rev. E* **94** , 032403 (2016)

[59] Rai, A. K., Rai, A., Ramaiya, A. J., Jha, R. & Mallik, R. Molecular adaptations allow Dynein to generate large collective forces inside cells. *Cell* **152**, 172-182 (2013)

[60] Schnitzer, M. J., Visscher, K. & Block, S. M. Force production by single kinesin motors, *Nat. Cell. Biol.* **2**, 718-723 (2000)

[61] Mallik, R., Petrov, D., Lex, S. A., King, S. J. & Gross, S. P. Building complexity: an in vitro study of sytoplasmic dynein with in vivo implications. *Curr. Biol.* **15**, 2075-2085 (2005)

[62] Toba, S. *et al.* Overlapping hand-over-hand mechanism of single molecular motility of cytoplasmic dynein. *Proc. Natl. Acad. Sci.* **103**, 5741-5745 (2006)

[63] Beeg, J. *et. al* Transport of beads by several kinesin motors. *Biophys. J.* **94** 532-541 (2008)

[64] Leduc, C. *et.al.* Cooperative extraction of membrane nanotubes by molecular motors. *Proc. Natl. Acacd. Sci.* **101** 17096-17101 (2004)

[65] Reck-Peterson, S. L. *et.al.* Single-molecule analysis of dynein processivity and stepping behaviour. *Cell* **126**, 335-348 (2006)

[66] Carter, N. J. & Cross, R. A. Mechanics of kinesin step. *Nature* **435**, 308-312 (2005)

[67] King, S. J. & Schroer. T. A. Dynactin increases the processivity of cytoplasmic dynein motor. *Nat. Cell. Biol* **2** 20-24 (2000)

[68] Kojima, H., Kikumoto, M., Sakakibara, H. and Oiwa, K. Mechanical Properties of a Single-Headed Processive Motor, Inner-Arm Dynein Subspecies-c of Chlamydomonas Studied at the Single Molecule Level. *J. Biol. Phys.* **28** 335-345 (2002)

[69] Gennerich, A., Carter, A. P., Reck-Peterson, S. L. and Vale, R. D., Force-Induced Bidirectional Stepping of Cytoplasmic Dynein, *Cell* **131**, 952-965 (2007)

[70] Gillespie, D. T. A general method for numerically simulating the stochastic time evolution of coupled chemical reactions *Journal of Computational Physics* **22** 403434 (1976)

[71] Gillespie, D. T. Exact stochastic simulation of coupled chemical reactions *J. Phys. Chem.* **81**, 2340-2361 (1977)

[72] Narayanan, T. and Kumar, A. Reentrant phase transitions in multicomponent liquid mixtures *Phys. Rep.* **249**, 135-218 (1994)

[73] Saxton, W. M., Hicks, J., Goldstein, L. S. and Raff, E. C. Kinesin heavy chain is essential for viability and neuromuscular functions in Drosophila, but mutants show no defects in mitosis. *Cell* **64**, 1093 (1991)

[74] Hurd, D. D. and Saxton, W. M. Kinesin mutations cause motor neuron disease phenotypes by disrupting fast axonal transport in Drosophila. *Genetics* **144**, 1075 (1996)

[75] Gindhart, J. G., Desai, C. J., Beushausen, S., Zinn, K. and Goldstein, L. S. Kinesin light chains are essential for axonal transport in Drosophila. *J. Cell Biol.* **141**, 443 (1998)

[76] Gross, S. P. Dynactin: coordinating motors with opposite inclinations. *Curr. Biol.* **13**, R320R322 (2003)

[77] Gross, S. P. Hither and yon: a review of bi-directional microtubule-based transport. *Phys. Biol.* **1**, R1R11 (2004)

[78] Gross, S. P., Guo, Y., Martinez, J. E. and Welte, M. A. A determinant for directionality of organelle transport in Drosophila embryos. *Curr. Biol.* **13**, 16601668 (2003)

[79] Gross, S. P., Welte, M. A., Block, S. M. and Wieschaus, E. F. Dynein-mediated cargo transport *in vivo.* A switch controls travel distance. *J. Cell Biol.* **148**, 945956 (2000)

[80] Shubeita, G. T., Tran, S. L., Xu, J., Vershinin, M., Cermelli, S., Cotton, S. L., Welte, M. A. and Gross, S. P. Consequences of motor copy number on the intracellular transport of kinesin-1-driven lipid droplets. *Cell* **135**, 10981107 (2008)

[81] Welte, M. A., Cermelli, S., Griner, J., Viera, A., Guo, Y., Kim, D. H., Gindhart, J. G. and Gross, S. P. Regulation of lipid-droplet transport by the perilipin homolog LSD2. *Curr. Biol.* **15**, 12661275 (2005)

[82] McKenney, R. J., Vershinin, M., Kunwar, A., Vallee, R. B. and Gross, S. P. LIS1 and NudE induce a persistent dynein force-producing state. *Cell* **141**, 304314 (2010)

[83] Roos, W. H., Campas, O., MOntel, F., Woehlke, G., Spatz, J. P., Bassereau, P. and Cappello, G. Dynamic kinesin-1 clustering on microtubules due to mutually attractive interactions. *Phys. Biol.* **5**, 1-10 (2008)

[84] Gu, Y., Sun, W., Wang, G., Jeftinija, K., Jeftinija, S. and Fang, N. Rotational dynamics of cargos at pauses during axonal transport. *Nature Commun.* **3**, 1030 (2012)

[85] Kolomeisky, A. B. Motor proteins and molecular motors: how to operate machines at the nanoscale. *P. Phys: Cond. Mat.* **25**, 463101 (2013)

[86] Mallik, R., Carter, B. C., Lex, S. A., King, S. J. and Gross, S. P. Cytoplasmic dynein functions as a gear in response to load. *Nature* **427**, 649-652 (2004)

[87] Singh, M. P., Mallik, R., Gross, S. P., Clare, C. C. Monte Carlo modeling of single-molecule cytoplasmic dynein. *Proc. Nat. Acad. Sci. USA* **102**, (2005)